Supplement of Atmos. Chem. Phys., 19, 14071–14090, 2019
https://doi.org/10.5194/acp-19-14071-2019-supplement

Atmospheric Chemistry and Physics
Open Access
EGU

Supplement of

Novel approaches to improve estimates of short-lived halocarbon emissions during summer from the Southern Ocean using airborne observations

Elizabeth Asher et al.

Correspondence to: Elizabeth Asher (elizabeth.asher@noaa.gov)

Supplementary Text

Sea air exchange calculations

To support the interpretation of our results, we calculate nominal equilibration times. For estimates of bulk sea air equilibration times for halogenated VOCs, O_2, and CO_2, we assume a mixed layer depth of 30 m, a temperature of 0° C, a salinity of 35 PSU, and carbonate buffering according to eq. 8.3.10 in Sarmiento and Gruber (2006), and transfer velocities according to Nightingale et al., (2000). The Schmidt number (i.e. the ratio of the kinematic viscocity of a gas, divided by the molecular diffusivity) for O_2, CO_2 and CH_3Br were calculated according to Wanninkof (2014), and the Schmidt numbers for $CHBr_3$ and CH_3I were calculated according to Quack and Wallace (2003) and Moore and Groszko (1999), respectively. The results are provided in Sect. 3.1.2.

Comparisons of TOGA, WAS and PFP

Despite overall good agreement between co-located inflight AWAS, WAS, and PFP samples and TOGA measurements, we observed notable discrepancies in several cases (e.g. Fig. S1b; Fig. S2a-b). On ORCAS, we observed a non-linear relationship between inflight TOGA measurements and co-located AWAS samples of CH_3I (Fig. S1b), driven by a few samples with high mixing ratios. Close inspection of upwind and downwind flights over Region 2 with the campaign's high mixing ratios of CH_3I indicated that TOGA measurements were consistent with a modest flux of CH_3I from the ocean to the atmosphere. On ATom-2, TOGA measurements agreed better with co-located PFP samples than with co-located WAS samples; and differences on the sixth and seventh research flights (i.e. the data used here) were relatively small. Nevertheless these differences motivated an instrument inter-comparison following the ATom campaign between these instruments. Thus far, results of this inter-comparison show that TOGA and PFP measurements differ by < 25%.

Supplementary Tables

Table S1. The TOGA-PFP instrument comparison was done by sampling a 50L SS pontoon, created at NCAR from a humidified dilution of the TOGA ATom standard. Data were analyzed and reported by Rebecca Hornbrook (NCAR, TOGA) and Steve Montzka (NOAA, PFP).

Pontoon Inter-comparison	Concentration (dilution-based calc.)	TOGA (10/12/2018)	PFP (10/24/2018)
$CHBr_3$	34	21.0 ± 0.1	26.6 ± 0.8
$CHClBr_2$	26	19.9 ± 1.0	22.9 ±0.1
CH_2Br_2	52	47.7 ± 0.2	51.7 ± 2.0

Supplementary Figures

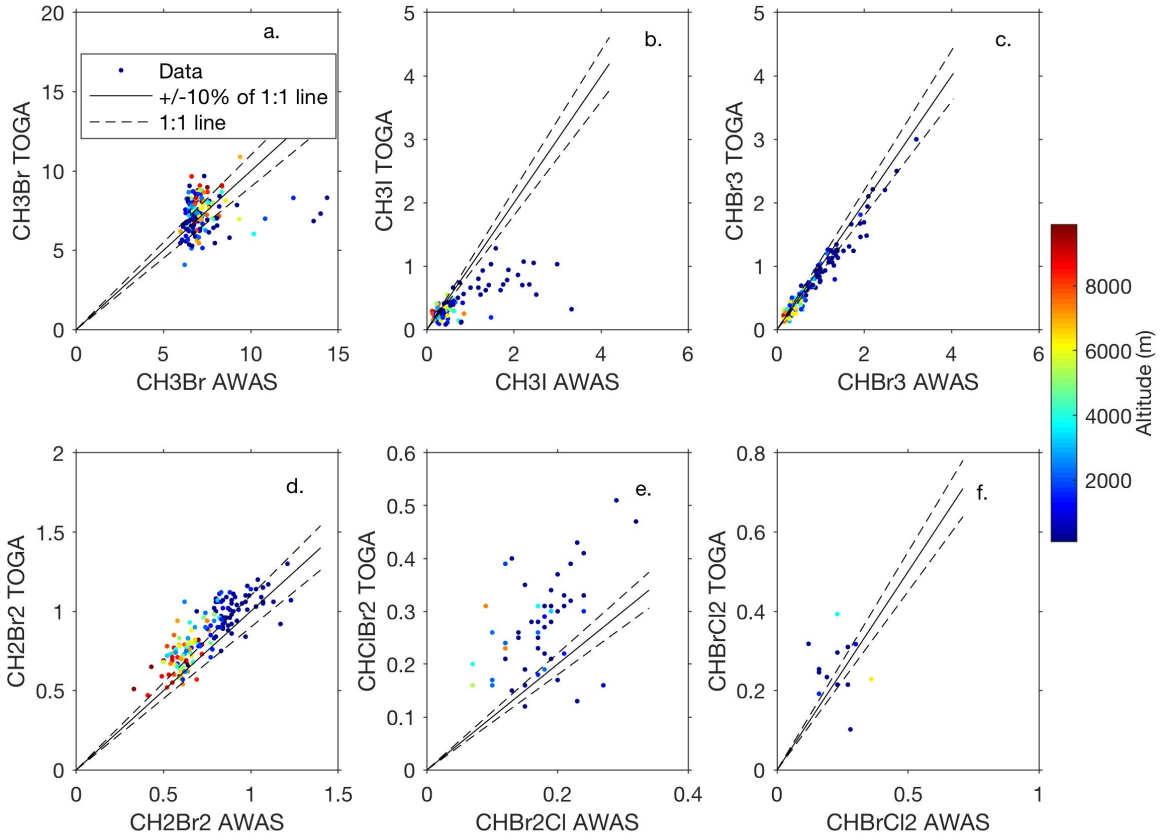

Figure S1. Comparison between AWAS samples and TOGA measurements during ORCAS below 10 km, when these two shared over half their sampling period Points are colored by altitude. Dashed lines represent ± 10% of the 1:1 line. Sample points below the DL are not included in this quantitative comparison.

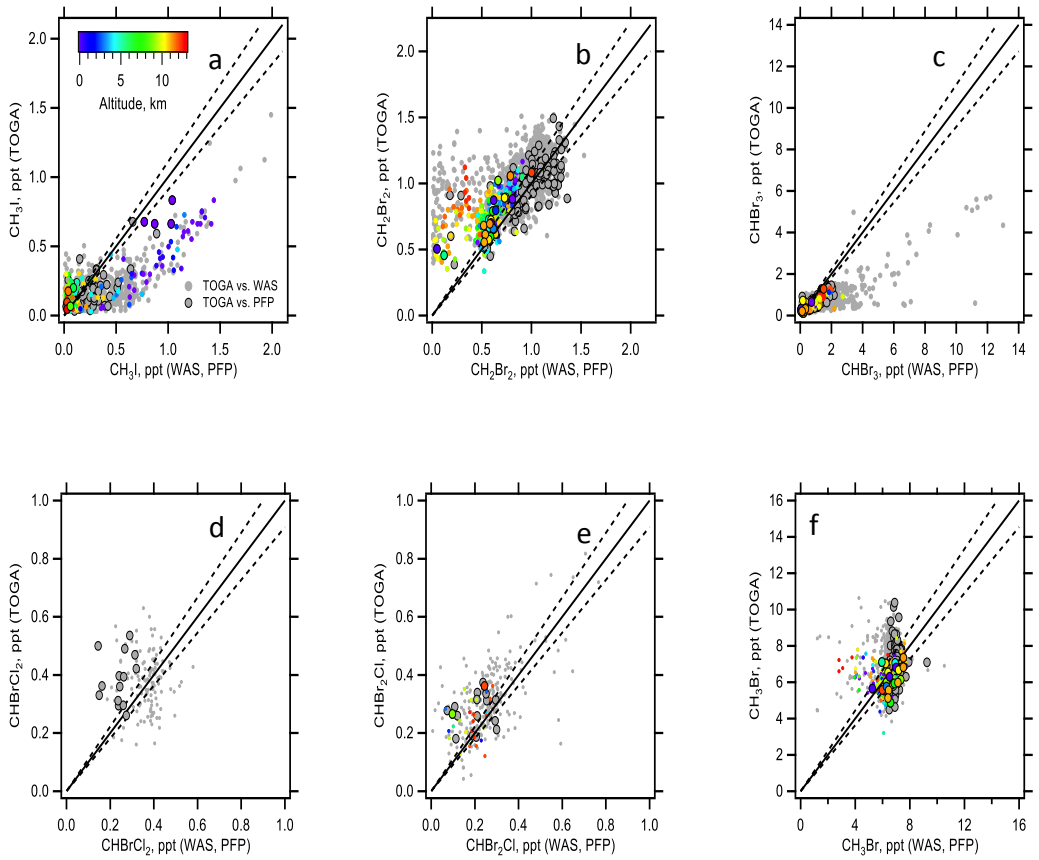

Figure S2. Comparison between WAS, PFP and TOGA measurements during ATom-2 below 10 km, when these instruments shared over half their sampling period. WAS measurements are shown in larger circles, PFP measurements in smaller circles, and measurements from the research flights six and seven used in this analysis are shown in color, while measurements on other research flights in ATom-2 are shown in gray. Dashed lines represent ± 10% of the 1:1 line. Sample points below the DL are not shown.

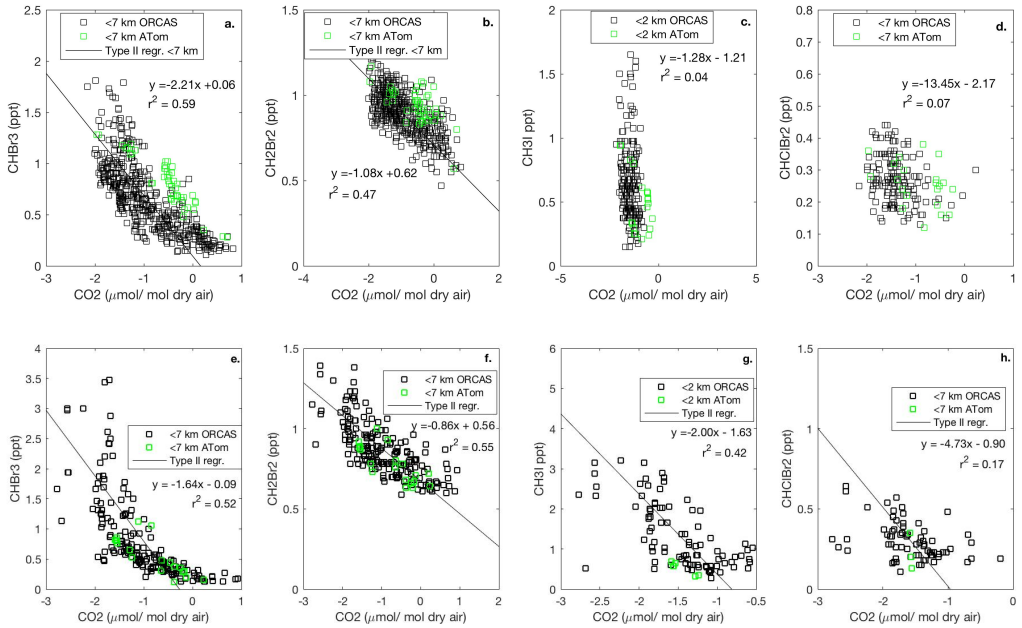

Figure S3. Mixing ratios of $CHBr_3$, CH_2Br_2 and CH_3I vs. CO_2 in Region 1 (a-c) and Region 2 (d-f). Type II major axis regression model (bivariate least squares regression) fits are shown for combined ORCAS and ATom-2 data, using data below 7 km for $CHBr_3$, CH_2Br_2, and below 2 km for CH_3I.

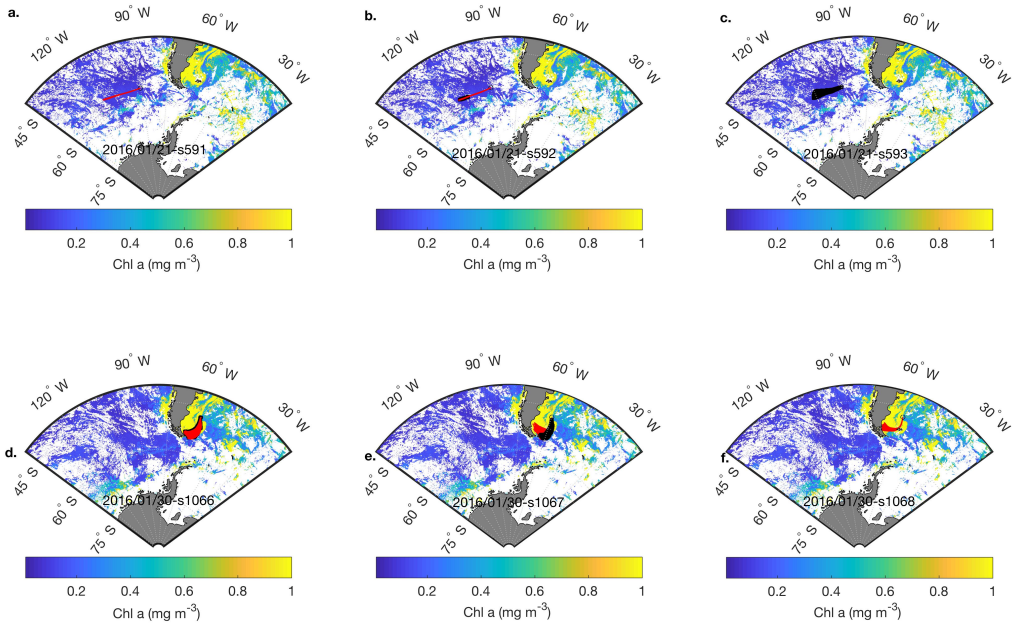

Figure S4. Two sets of three consecutive TOGA VOC sample locations, their back-trajectories and surface influences in the lower troposphere on two different flights (a-c; Jan. 21,2016, and d-f; Jan. 30, 2016). For illustrative purposes, sampling locations are denoted by a black circle, 24-hour back trajectories are shown in red, and surface influences are shown with black squares in each subpanel, overlying weekly composites of remotely sensed chl *a*. Surface influence is multiplied by the underlying chl *a* (or other) surface field and averaged for each sample to yield a surface influence function.

References

Sarmiento, J., Gruber, N., & McElroy, M. (2007). Ocean Biogeochemical Dynamics. *Physics Today*, *60*, 65. https://doi.org/10.1063/1.2754608

Wanninkhof, R. (2014). Relationship between wind speed and gas exchange over the ocean revisited: Gas exchange and wind speed over the ocean. *Limnology and Oceanography: Methods*, *12*(6), 351–362. https://doi.org/10.4319/lom.2014.12.351